Published in final edited form as:
*Science*. 2010 May 7; 328(5979): 757–760. doi:10.1126/science.1186743.

# Sequential Checkpoints Govern Substrate Selection During Cotranslational Protein Targeting

**Xin Zhang**[1], **Rumana Rashid**[1,2], **Kai Wang**[3], and **Shu-ou Shan**[1,*]

[1]Division of chemistry and chemical engineering, California Institute of Technology, 1200 E. California Blvd., Pasadena, CA 91125, USA

## Abstract

Proper protein localization is essential for all cells. However, the precise mechanism by which high fidelity is achieved is not well understood for any targeting pathway. To address this fundamental question we investigated the signal recognition particle (SRP) pathway in *E. coli*, which delivers proteins to the bacterial inner membrane through recognition of signal sequences on cargo proteins. Fidelity was thought to arise from the inability of SRP to bind strongly to incorrect cargos. Using biophysical assays, we found that incorrect cargos were also rejected through a series of checkpoints during subsequent steps of targeting. Thus high fidelity is achieved through the cumulative effect of multiple checkpoints; this principle may be generally applicable to other pathways involving selective signal recognition.

Co-translational protein targeting is an essential and evolutionarily conserved pathway for delivering proteins to the proper cellular membrane (1, 2). Targeting begins when the signal recognition particle (SRP) recognizes an N-terminal signal sequence on its cargo, a translating ribosome bearing a nascent polypeptide chain (RNC) (Fig. 1A, step 1) (1–6). Cargo-loading facilitates efficient interaction between the GTPase domains of both the SRP and SRP receptor (SR), and stabilizes the SRP-SR complex in an early conformational state (step 2) (7, 8). The interactions of SR with the target membrane and the protein conducting channel is proposed to induce dynamic rearrangements in the SRP-SR complex (4, 6, 8), first to form a GTP-dependent closed complex (step 3) and then to activate GTP hydrolysis in the complex (step 4). These rearrangements facilitate the unloading of cargo from SRP to the translocation machinery (steps 3–4) (4, 6, 8). In a productive targeting cycle, GTP is hydrolyzed after cargo unloading to drive the disassembly and recycling of SRP and SR (step 5) (9).

How SRP ensures faithful delivery of correct cargos remains poorly understood. The SRP signal sequences are highly degenerate, and their differences from the signal sequences of non-SRP substrates are minor (10). Thus SRP must have evolved a strategy to remain highly specific to its substrates despite the 'noise' in its recognition signal. 'Incorrect' cargos were thought to be rejected because they bind weakly to the SRP (11; Fig. 1A, arrow a). To test this hypothesis, we systematically varied the signal sequence based on alkaline phosphatase (phoA) (10, 12, 13). We replaced the hydrophobic core of the phoA signal sequence (Fig. 1B) with a combination of leucine and alanine, and varied the Leu/Ala ratio to generate signal sequences with different hydrophobicity (12, 13). Another incorrect cargo is the *E. coli* autotransporter EspP. Although EspP contains a signal sequence with hydrophobicity

*To whom correspondence should be addressed. sshan@caltech.edu.
[2]Current address: Department of Molecular Medicine, City of Hope, 1500 East Duarte Road, Duarte, California 91010, USA
[3]Current address: WongPartnership LLP, One George Street, #20-01, Singapore 049145

**Supporting Online Material**: Materials and Methods, Supplementary text, Figures S1 to S9, and references.

comparable to that of phoA-3A7L, it is not an SRP substrate due to an N-terminal extension (Fig. 1B) (14). Firefly luciferase, a cytosolic protein without signal sequences, was used as a negative control (Fig. 1B) (12). For all the experiments, homogeneous stalled RNCs were purified and used as cargos (8, 15).

We first tested the binding affinities of SRP for different cargos (Fig. 1A, step 1). RNC binding to SRP was detected as an increase in the fluorescence anisotropy of fluorescein-labeled SRP (C421). Cargos with the most hydrophobic signal sequences bound to SRP tightly ($RNC_{1A9L}$ and $RNC_{2A8L}$), with equilibrium dissociation constants ($K_d$) of ~1 nM or less (Figs. 1C and S1). The next strongest cargo, $RNC_{3A7L}$, also exhibited strong albeit attenuated binding to SRP, with $K_d$ ~ 10 nM (Fig. 1C). Nevertheless, the affinity of incorrect cargos or the empty ribosome for SRP was still substantial, with $K_d$'s of 80 – 100 nM (Fig. 1, D–E, and fig. S1; see also ref 16). At the cellular SRP concentration of ~400 nM (Fig. 1E) (17), a substantial amount of incorrect cargos could bind to SRP (18). Surprisingly, although EspP is not an SRP substrate, $RNC_{EspP}$ bound SRP as tightly as $RNC_{3A7L}$ (Fig. 1C). Thus the differences in cargo binding affinity do not provide sufficient discrimination against incorrect cargos, and additional factors in the bacterial cytosol did not increase the specificity of SRP-cargo binding (Fig. S2 and SOM text) (19). We therefore proposed that subsequent steps in the targeting pathway, including formation of the SRP-SR complex and GTP hydrolysis, provide additional checkpoints to reject the incorrect cargos (Fig. 1A, red arrows b–d and SOM text) (20).

We first tested whether the early SRP-SR complex is stabilized more strongly by the correct than the incorrect cargo (Fig. 1A, arrow b). We assembled cargo-SRP-SR early complexes in the absence of nucleotides; this blocks the rearrangement of the GTPase complex to subsequent conformations (7, 8). The equilibrium stabilities of the early complexes were measured using fluorescence resonance energy transfer (FRET) between donor- and acceptor-labeled SRP and SR (7). The early complex was significantly stabilized by $RNC_{1A9L}$ and $RNC_{2A8L}$, with $K_d$ ~ 80 nM (Fig. 2A), and this stability was weakened up to 50-fold for the weaker cargos (Fig. 2, B–C, and fig. S3). With incorrect cargos such as $RNC_{EspP}$ and $RNC_{luciferase}$, the FRET efficiency also plateaued at lower values, ~0.3 – 0.4 (Fig. 2, B and D, and fig. S3), compared to ~0.66 with the correct cargos (Fig. 2, A and D). This suggests that the SRP and SR are likely positioned differently in the early targeting complexes formed by the incorrect cargos.

A mispositioned early complex would lead to a slower rearrangement to form the closed complex (Fig. 1A, step 3). To test this hypothesis, we preformed the early targeting complex and directly measured its rearrangement using acrylodan-labeled SRP (C235), which specifically monitors the closed complex. With $RNC_{1A9L}$, this rearrangement occurred at 0.3 $s^{-1}$ (Fig. 2E). $RNC_{3A7L}$ and $RNC_{phoA}$ mediated this rearrangement 40% slower (Fig. 2G and S4). Notably, $RNC_{EspP}$ and cargos weaker than $RNC_{5A5L}$ mediated this rearrangement 5–10-fold slower than $RNC_{1A9L}$ (Fig. 2, F–G, and fig. S4). Thus incorrect cargos do not induce the formation of a stable and productive early complex, and are more likely to exit the pathway (Fig. 1A, arrow b).

The more favorable pre-equilibrium to form the early intermediate combined with the faster early-to-closed rearrangement would allow the correct cargos to mediate faster GTP-dependent assembly of a stable closed complex (Fig. 1A, steps 2–3). We characterized this cumulative effect using both FRET (Fig. 3, A–C, and fig. S5, F–G) and acrylodan-labeled SRP (C235) (Fig. S5). Both probes showed that the correct cargos mediated rapid assembly of the closed complex (Fig. 3A and S5A), and this rate decreased significantly with weaker signal sequences (Fig. 3, B–C, and fig. S5). Overall, there is a ~$10^3$-fold kinetic

discrimination between the strongest and weakest cargos in stable SRP-SR complex assembly, which delivers the cargo to the membrane (Fig. 3C and S5E).

If GTP hydrolyzed too quickly in the SRP-SR complex, this would abort the targeting reaction before the cargo is productively unloaded (8, 21). To test whether the correct cargos prevent premature GTP hydrolysis better than the incorrect cargos (Fig. 1A, step 4), we determined the GTPase rates from the cargo-SRP-SR complex. $RNC_{1A9L}$ and $RNC_{2A8L}$ reproducibly delayed GTP hydrolysis 6–8 fold (Fig. 3D and S6). $RNC_{3A7L}$ had a 3–4 fold inhibitory effect on the GTPase reaction (Fig. S6). In contrast, incorrect cargos such as $RNC_{EspP}$ did not substantially affect the GTPase rate (Fig. 3, E–F, and fig. S6). Thus the fidelity of protein targeting can be further improved through kinetic proofreading mechanisms by using the energy of GTP hydrolysis (Fig. 1A, arrow d).

Our data suggested a model in which the incorrect cargos are rejected not only through binding affinity, but also through differences in the kinetics of SRP-SR complex assembly and GTP hydrolysis (Fig. 1A and 4A, top). Based on this model, we calculated the amount of substrates retained in the SRP pathway after each checkpoint (SOM Methods). The cargo binding step was not sufficient to discriminate against incorrect cargos, allowing over 75% of them to enter the SRP pathway (Fig. 4A, light grey). During cargo delivery through SRP-SR complex assembly, a large fraction of substrates weaker than phoA were rejected (Fig. 4A, dark grey). Finally, kinetic competition between GTP hydrolysis and cargo unloading further improved the discrimination between correct and incorrect substrates (Fig. 4A, black). To validate the model, we determined the targeting efficiency of proteins with various signal sequences using a well-established assay that tests the ability of *E. coli* SRP and SR to mediate the co-translational targeting of preproteins to microsomal membranes (SOM Methods) (22, 23). Substrates with signal sequences stronger than 3A7L were efficiently targeted and translocated (Fig. 4B and S7). In contrast, EspP and substrates with signal sequences weaker than phoA showed severe defects in translocation, and almost no translocation was detected for phoA-8A2L (Fig. 4B). The experimentally determined protein targeting efficiencies agreed well with predictions based on the kinetic and thermodynamic measurements (Fig. 4C), suggesting that our model (Fig. 1A and 4A) faithfully represents how SRP handles its substrates.

Thus fidelity during cotranslational protein targeting is achieved through the cumulative effect of multiple checkpoints, by using a combination of binding, induced fit, and kinetic proofreading mechanisms (SOM text). Although the incorrect cargos are not completely rejected during the initial binding step, they are discriminated repeatedly during subsequent steps possibly because they bind the SRP in a less productive mode (6). In addition, the translocation machinery provides another important checkpoint (24). Similar strategies of using multiple checkpoints to ensure fidelity have been demonstrated in tRNA synthetases (25), protein synthesis (26), and DNA and RNA polymerases (27, 28), and possibly represent a general principle for complex cellular pathways that need to recognize degenerate signals or to discriminate between correct and incorrect substrates based on minor differences.

## Supplementary Material

Refer to Web version on PubMed Central for supplementary material.

## Acknowledgments

We thank C. Schaffitzel and N. Ban for help with the purification of RNCs and TF, J. Luirink for plasmids encoding the phoA signal sequence variants, L. Randall for the plasmid encoding luciferase, B. Bukau and E. Deuerling for the plasmid encoding TF, H.D. Bernstein for the strain HDB51, and R.J. Deshaies, A. Varshavsky,

W. Zhong, N. Pierce, and the Shan laboratory for comments on the manuscript. This work was supported by NIH grant GM078024, and career awards from the Burroughs Welcome Foundation, the Henry and Camille Dreyfus foundation, the Beckman foundation, and the Packard foundation to S.S.

## References and Notes

1. Walter P, Johnson AE. Annu. Rev. Cell Biol. 1994; 10:87. [PubMed: 7888184]
2. Rapoport TA. Nature. 2007; 450:663. [PubMed: 18046402]
3. Halic M, et al. Nature. 2006; 444:507. [PubMed: 17086193]
4. Halic M, et al. Science. 2006; 312:745. [PubMed: 16675701]
5. Schaffitzel C, et al. Nature. 2006; 444:503. [PubMed: 17086205]
6. Pool MR, Stumm J, Fulga TA, Sinning I, Dobberstein B. Science. 2002; 297:1345. [PubMed: 12193787]
7. Zhang X, Kung S, Shan SO. J. Mol. Biol. 2008; 381:581. [PubMed: 18617187]
8. Zhang X, Schaffitzel C, Ban N, Shan SO. Proc. Natl. Acad. Sci. U. S. A. 2009; 106:1754. [PubMed: 19174514]
9. Connolly T, Gilmore R. Cell. 1989; 57:599. [PubMed: 2541918]
10. Huber D, et al. J. Bacteriol. 2005; 187:2983. [PubMed: 15838024]
11. De Gier JW, Valent QA, Von Heijne G, Luirink J. FEBS Lett. 1997; 408:1. [PubMed: 9180256]
12. Valent QA, et al. EMBO J. 1995; 14:5494. [PubMed: 8521806]
13. Doud SK, Chou MM, Kendall DA. Biochemistry. 1993; 32:1251. [PubMed: 8448135]
14. Peterson JH, Szabady RL, Bernstein HD. J. Biol. Chem. 2006; 281:9038. [PubMed: 16455668]
15. Schaffitzel C, Ban N. J. Struct. Biol. 2007; 158:463. [PubMed: 17350284]
16. Bornemann T, Jockel J, Rodnina MV, Wintermeyer W. Nat. Struct. Mol. Biol. 2008; 15:494. [PubMed: 18391966]
17. Jensen CG, Pedersen S. J. Bacteriol. 1994; 176:7148. [PubMed: 7525539]
18. Flanagan JJ, et al. J. Biol. Chem. 2003; 278:18628. [PubMed: 12621052]
19. Buskiewicz I, et al. Proc. Natl. Acad. Sci. U. S. A. 2004; 101:7902. [PubMed: 15148364]
20. Zheng N, Gierasch LM. Cell. 1996; 86:849. [PubMed: 8808619]
21. Miller JD, Bernstein HD, Walter P. Nature. 1994; 367:657. [PubMed: 8107852]
22. Powers T, Walter P. EMBO J. 1997; 16:4880. [PubMed: 9305630]
23. Shan SO, Chandrasekar S, Walter P. J. Cell Biol. 2007; 178:611. [PubMed: 17682051]
24. Hegde RS, Kang SW. J. Cell Biol. 2008; 182:225. [PubMed: 18644895]
25. Fersht AR, Kaethner MM. Biochemistry. 1976; 15:3342. [PubMed: 182209]
26. Rodnina MV, Wintermeyer W. Annu. Rev. Biochem. 2001; 70:415. [PubMed: 11395413]
27. Kunkel TA, Bebenek K. Annu. Rev. Biochem. 2000; 69:497. [PubMed: 10966467]
28. Uptain SM, Kane CM, Chamberlin MJ. Annu. Rev. Biochem. 1997; 66:117. [PubMed: 9242904]

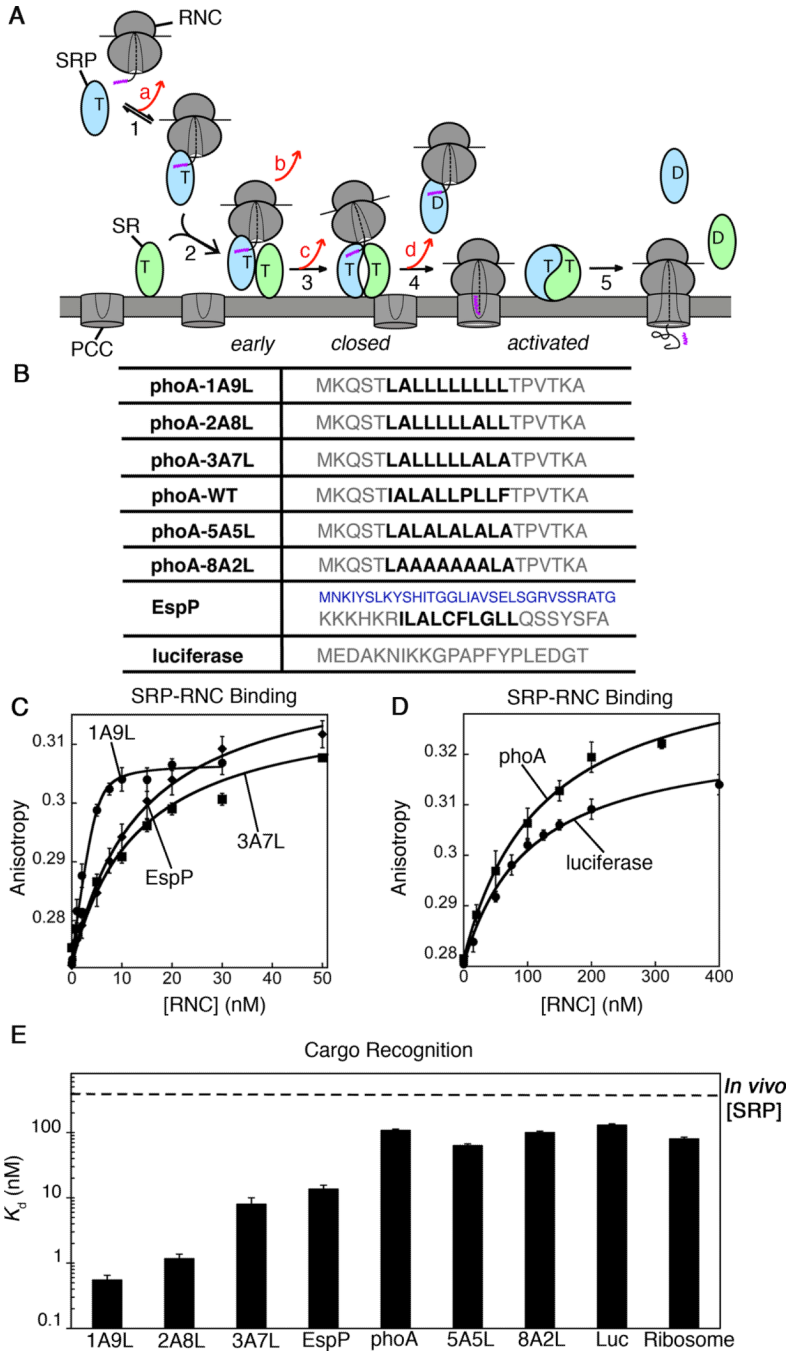


**Figure 1. Potential fidelity checkpoints in the SRP pathway**

(A) Model for potential checkpoints during co-translational protein targeting. A cargo (RNC) with a signal sequence (magenta) enters the pathway upon binding SRP, and is either retained (black arrows) or rejected (red arrows) at each step (numbered 1–5). T and D denote GTP and GDP, respectively. (B) Signal sequence variants used in this study. Bold highlights the hydrophobic core. Blue highlights the N-terminal signal sequence extension of EspP. (C, D) Equilibrium titrations of SRP-RNC binding. Nonlinear fits of data gave $K_d$ values of 0.55±0.20, 8.4±2.0, 13.6±3.0, 108±11 and 130±12 nM for $RNC_{1A9L}$ (C, ●), $RNC_{3A7L}$ (C, ■), $RNC_{EspP}$ (C, ◆), $RNC_{phoA}$ (D, ■) and $RNC_{luciferase}$ (D, ●), respectively. Error bars are SDs from three independent experiments. (E) Summary of the binding

affinities of SRP for different cargos. The dashed line denotes the cellular SRP concentration of 400±58 nM. Error bars are SEs of the fits.

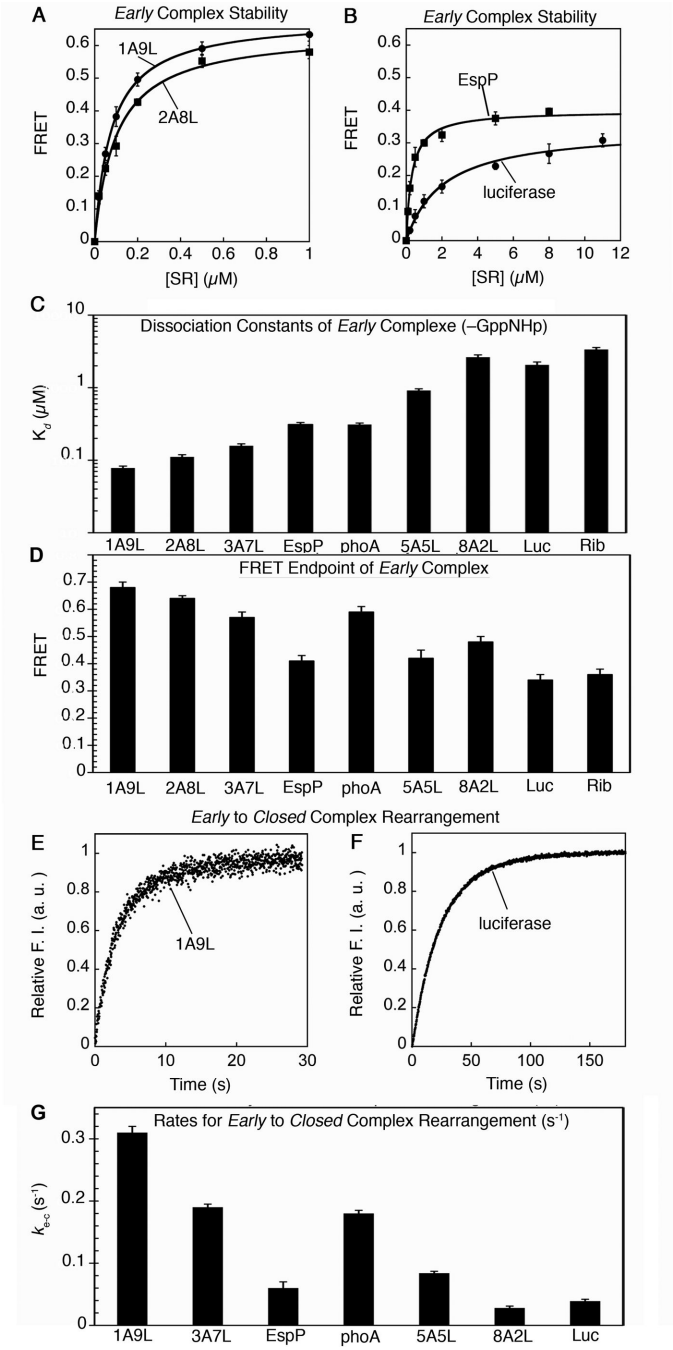


**Figure 2. Correct cargos stabilize the early intermediate and mediate faster rearrangement to the closed complex**

(A, B) Equilibrium titrations of the early intermediate. Nonlinear fits of data gave $K_d$ values of 78±5, 110±8, 311±21 and 2060±201 nM and FRET endpoints of 0.68±0.02, 0.64±0.02, 0.41±0.03, and 0.34±0.02 for $RNC_{1A9L}$ (A, ●), $RNC_{2A8L}$ (A, ■), $RNC_{EspP}$ (B, ■), and $RNC_{luciferase}$ (B, ●), respectively. Error bars are SDs from three independent experiments. (C, D) Summary of the $K_d$ values (C) and FRET end points (D) of the early intermediates formed by different cargos. Error bars are SEs of the fits in C and SDs from three independent experiments in D. (E, F) Measurements of the early to closed rearrangement. Nonlinear fits of data gave rate constants of 0.31±0.02 $s^{-1}$ with $RNC_{1A9L}$ (E) and

$0.039\pm0.003\ s^{-1}$ with $RNC_{luciferase}$ (F). Error bars are SDs from three independent experiments. (G) Summary of the rate constants for the early to closed rearrangement with different cargos. Error bars are SEs of the fits.

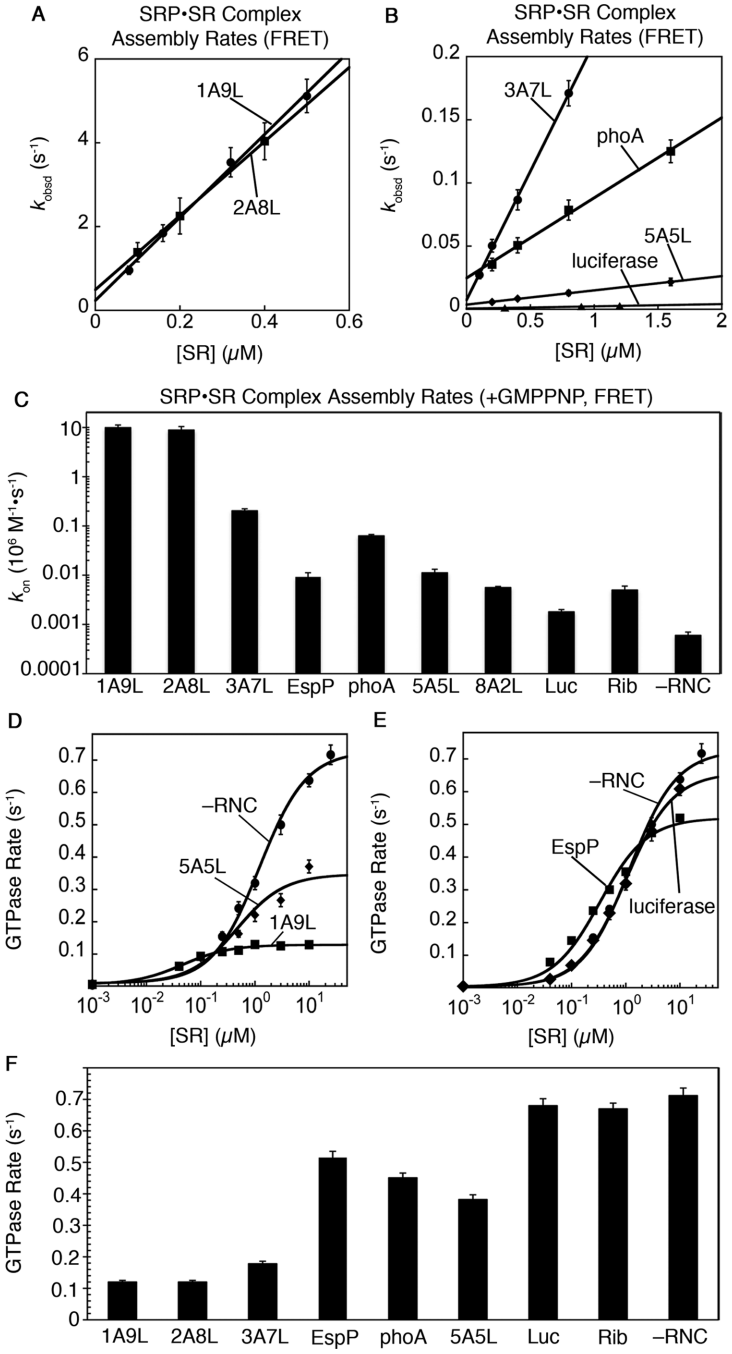


**Figure 3. Correct cargos accelerate GTP-dependent complex formation but delay GTP hydrolysis**

(A, B) Rate constants of SRP-SR complex assembly in GMPPNP measured by FRET. Linear fits of data gave $k_{on}$ values of $9.9\pm1.3\times10^6$, $8.8\pm1.6\times10^6$, $2.0\pm0.2\times10^5$, $6.3\pm0.4\times10^4$, $1.1\pm0.2\times10^4$ and $1.8\pm0.3\times10^3$ $M^{-1}s^{-1}$ for $RNC_{1A9L}$ (A, ●), $RNC_{2A8L}$ (A, ■), $RNC_{3A7L}$ (B, ●), $RNC_{phoA}$ (B, ■), $RNC_{5A5L}$ (B, ◆) and $RNC_{luciferase}$ (B, ▲), respectively. Error bars are SDs from three independent experiments. (C) Summary of GTP-dependent complex assembly rate constants with different cargos. Error bars are SEs of the fits. (D, E) Effects of cargo on GTP hydrolysis from the SRP•SR complex. Nonlinear fits of the data gave maximal GTPase rate constants ($k_{cat}$) of $0.72\pm0.03$ $s^{-1}$ without cargo (●), and $0.11\pm0.01$,

0.38±0.02, 0.51±0.08, and 0.65±0.22 $s^{-1}$ with $RNC_{1A9L}$ (D, ■), $RNC_{5A5L}$ (D, ◆), $RNC_{EspP}$ (E, ■) and $RNC_{luciferase}$ (E, ◆), respectively. Error bars are SDs from three independent experiments. (F) Summary of GTPase rate constants in the presence of different cargos. Error bars are SEs of the fits.

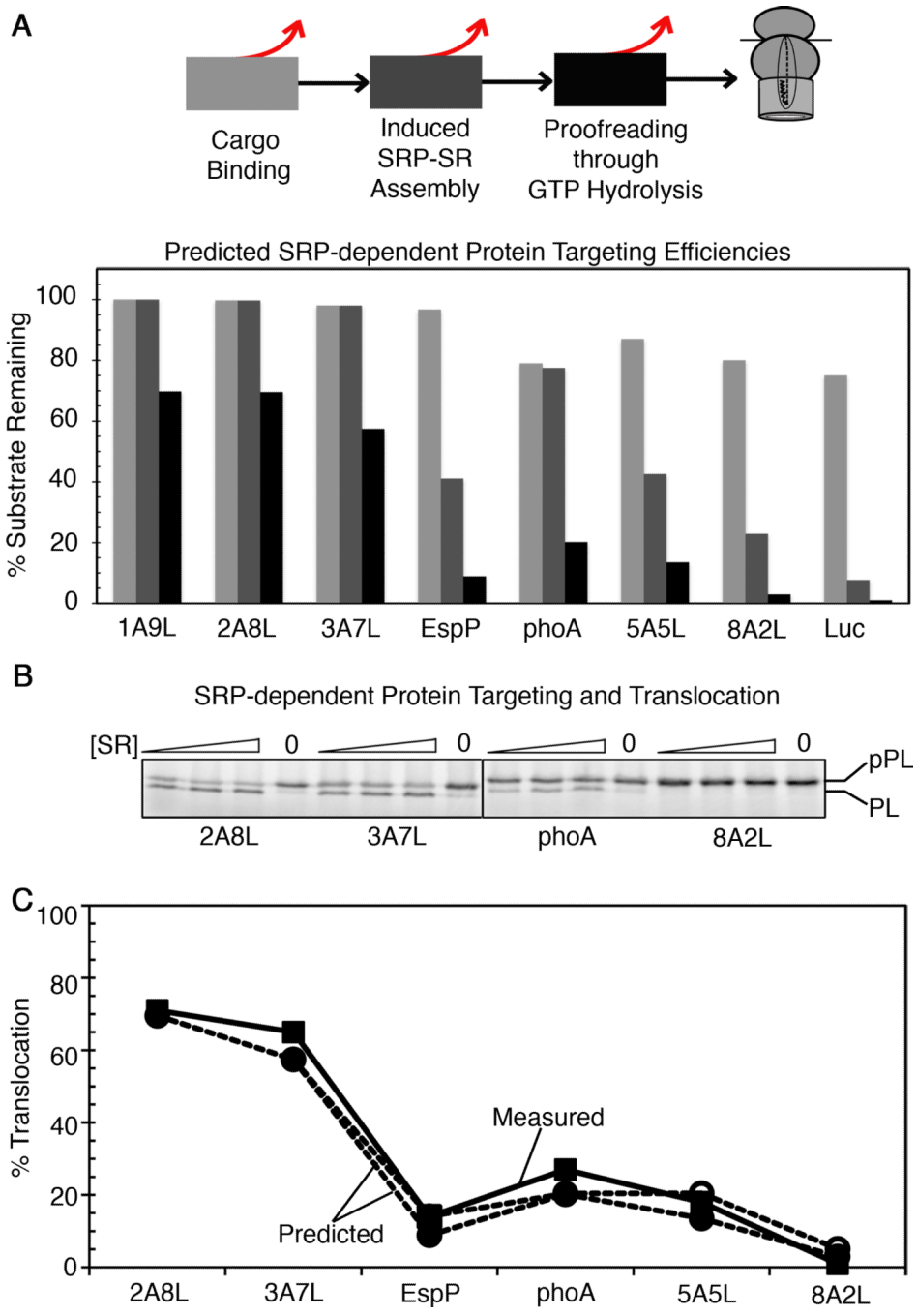


**Figure 4. Stepwise rejection of incorrect cargos from the SRP pathway**

(A) Top panel, cargos are either retained (black arrow) or rejected (red arrow) during each checkpoint. Lower panel, predicted fraction of cargos retained in the SRP pathway during each checkpoint (Supplementary text). (B) SRP-dependent protein targeting and translocation of the model substrates. pPL and PL denote the precursor and processed forms of the substrate, respectively. (C) Predicted protein targeting efficiencies (● and ○) agree well with the experimentally determined values (■), quantified from the data in (B). Translation elongation rates of 20 (●) and 10 amino acids/s (○) were used for the *E. coli* and eukaryotic ribosomes, respectively, to calculate the targeting efficiencies.